Al-Furat Journal of Innovations in Electronics and Computer Engineering (FJIECE)
ISSN -2708-3985

Enhancing FSO Communication Performance with UAV Technologies

Zaid Jabbar Al-Allaq [1*], Wafaa M. R. Shakir [2]

[1]Al-Furat Al-Awsat Technical University, Electrical Department, Karbala 56001, Iraq. E-mail: zaid.obaid@atu.edu.iq

[2]Al-Furat Al-Awsat Technical University, Computer Systems Department, Babil 51015, Iraq. E-mail: inb.wfa@atu.edu.iq

[*]Corresponding author E-mail: zaid.obaid@atu.edu.iq

https://doi.org/10.46649/fjiece.v4.1.15a.25.3.2025

Abstract. *Integrating unmanned aerial vehicles (UAVs) into a relay-based free space optical (FSO) communication system has several blessings that incorporate dealing with turbulence-induced atmospheric scintillation due to their flexible mobility. This study extensively assesses a UAV-FSO system that is based on a decode-and-forward dual-hop strategy with multiple transmission sources. Through the incorporation of the Gamma-Gamma (GG) distribution to measure factors such as atmospheric losses, atmospheric turbulence, angle-of-arrival fluctuations, and pointing errors, a faithful formula for the probability density function (PDF) of the total channel gain is derived. A mathematical representation for the average bit error rate (BER) of the system is also derived and later on, validated through extensive Monte Carlo simulations. The simulation outcomes spotlight model robustness across a range of operational conditions. These results underline the enhanced efficiency and versatility of the UAV-assisted FSO systems that can manage various data sources, and consequently, they can be quite applicable in the case of surveillance and mobile network communications.*

Keywords: *FSO communication, UAVs relay, BER, Pointing Error.*

1. INTRODUCTION

The rapid advancements in wireless communication technologies, with an increasing demand for higher data rates, has placed into a substantial strain on the strained traditional radio frequency (RF) communication systems resulting from an increasing need for higher data rates. In an effort to mitigate spectrum overcrowding, free space optical (FSO) communication has attracted considerable interest as a plausible substitute [1]-[3]. In contrast to RF communication systems, FSO technologies do not necessitate licensing, exhibit directional properties, are resistant to electromagnetic interference, and are difficult to intercept, rendering them particularly suitable for applications using line of sight (LoS) and wireless [4]-[6]. Terrestrial FSO systems face critical challenges despite these advantages, such as path loss, atmospheric turbulence, and pointing errors [7], [8]. Signals being sent through the air suffer random fluctuations in the received signal power that tend to become more and more severe as the transmission distance increases [9]. After getting over a few kilometers, the reliability of FSO communication signals decreases significantly [10]. Therefore, accuracy in LoS alignment is a crucial part of the system performance of FSO communications [11]. For dealing with these problems, relay-based FSO systems have been developed [12]. However, the existing solutions, particularly those of the fixed ground relays, like [13]-[19], have a limitation to adjust dynamically to the variable channel conditions. This imposes constraints on the practical application of the relays. Finding suitable locations for relays is a difficulty owing to multiple physical obstacles.

The evolution of technology in unmanned aerial vehicles (UAV) has been the cornerstone of the development of FSO wireless communication systems based on the UAV technology relay, as illustrated in [20], [21]. Through their dynamic repositioning in response to the changes in channel conditions, UAV-based FSO systems make LoS transmission requirements compatible by giving high mobility, and thus the overall communication performance is improved significantly [22]. The convergence of FSO with UAV technology will probably become the main force for the UAV communication systems upgrade throughout diverse applications [23]-[25].

A critical aspect of this development involves the creation of accurate channel models and performance metrics customized for UAV-assisted FSO relay systems. For example, studies on hybrid FSO/RF UAV-based have recently dealt with the problem of data throughput under buffering constraints [26]. However, the studies before [26]-[29] always have ignored the effect of the loss of the angle of arrival due to the change of the orientation of a UAVs. Reference [30] presented an innovative channel model for UAV-based FSO front-link, designed to account for angular fluctuations due to non-orthogonal laser beams. This model takes some input parameters into account. One of them is the misalignment of the beam and another one represents the changes in incidence angles, particularly occurring with weak atmospheric turbulence [31].

Moreover, surveys such as [32] have validated the dependability of FSO systems that operate at high altitudes, taking into account AoA fluctuations and misalignment-related losses. The recent improvements involve the incorporation of a full statistical channel model for FSO based on UAVs communication systems, taking into consideration atmospheric attenuation, turbulence, and pointing errors. Connectivity problems are also considered due to the variation of the AoA [33]. Nonetheless, the references [21], [33]-[39] mostly stick to the single-source systems; thus, multi-source configurations are generally left unexplored.

Incorporating multiple source nodes into UAV-assisted FSO systems presents significant practical benefits, particularly for applications like multipoint fire detection and cellular networks. This study focuses on a decode-and-forward (DF) dual-hop UAV-based FSO system and multiple sources, addressing the limitations of terrestrial fixed-relay systems [12]-[18]. Including UAV relays introduces greater mobility and adaptability while using multiple sources enhances system efficiency. This approach observes a considerable step forward in advancing the versatility and performance of UAV-enabled FSO communication networks.

This work introduces a novel analytical expression to derive the average BER for decode-and-forward relayed UAV-based FSO dual-hop systems. The proposed model that is being proposed will include explaining elements including pointing inaccuracies, arrival angle degradation, and atmospheric signal attenuation, employing a Gamma-Gamma (GG) distribution to model atmospheric turbulence. This framework explicitly addresses UAV-based free space optical systems include several source nodes and dual-hop decode-and-forward relays. Additionally, the probability density function (PDF) of the complete channel gain is derived and validated, providing a realistic and comprehensive model for system performance analysis.

The study is an exhaustive investigation of how the error probability behaves in various system and channel configurations, examining the atmospheric turbulence, misalignment, atmospheric losses, and AoA variations on performance. It also studies the advantages of using multiple source nodes to improve the operational mobility and flexibility of UAV-assisted FSO networks. Extensive Monte Carlo simulations confirm the theoretical results and provide significant insights into the rendition of UAV-

Al-Furat Journal of Innovations in Electronics and Computer Engineering (FJIECE)
ISSN -2708-3985

assisted FSO systems in different cases. Additionally, key system parameters are studied to suggest optimization strategies to enhance overall performance, underscoring the practical applicability of the proposed model.

The rest of the paper is structured as follows: Section II gives the system model. Section III focuses on the analysis of the system's performance. Section IV presents the numerical simulation results that align with the analytical conclusions, and Section V includes the conclusion.

2. SYSTEM MODEL

Illustrated in Figure 1 is the examination of a hovering UAV-based free space optical decode and forward dual hop system. This system comprises M source nodes $(S_1.S_2.,,,.S_M)$, a relay node (R) positioned on a hovering unmanned aerial vehicle, and a destination node (D) situated on a ground building. Within the system, a laser diode is employed as the transmitter (Tx) at every source node for the transmission of optical signals. It is presumed that the alignments of the Tx and the receiver (Rx) are synchronized with one another in every connection throughout the communication process. The unmanned aerial vehicle relay utilizes M optical antennas to receive optical signals and subsequently convert them into electrical signals. UAV relays are capable of offering a forwarding protocol within FSO networks similar to ground relays. Subsequently, the UAV relay consistently transmits optical signals utilizing the DF protocol. The receiving node at the destination utilizes a photodiode for signal reception and carries out the process of photoelectric conversion.

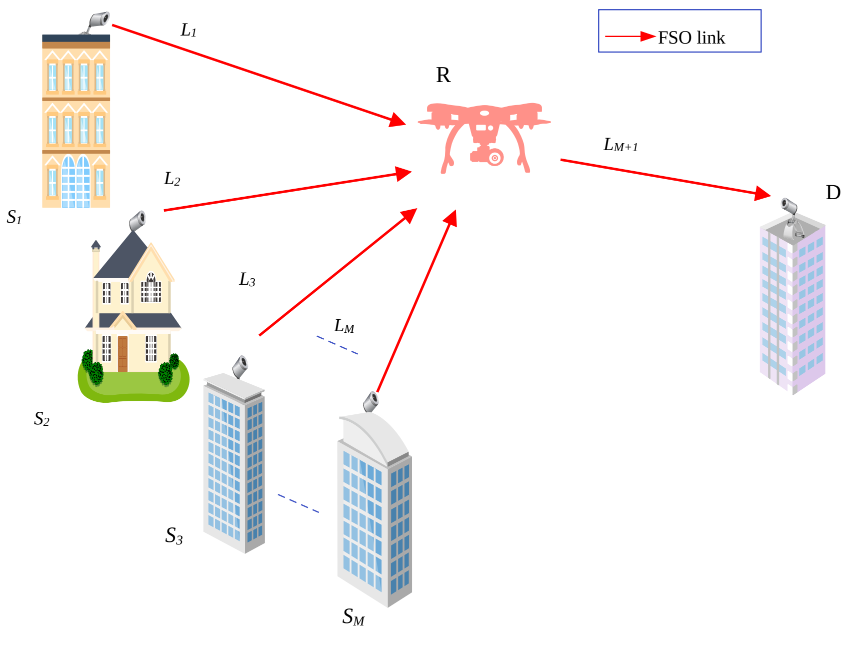

Fig. 1. The FSO relay system based on UAVs.

Al-Furat Journal of Innovations in Electronics and Computer Engineering (FJIECE)
ISSN -2708-3985

2.1. Received signal model

The communication links as a whole consist of two hops. In the initial hop, a total of M source nodes send out identical signal x_s to the unmanned aerial vehicles relay R. Subsequently, the signal that was obtained at node R may be written as

$$\mathrm{y_i} = \mathrm{GL_i x_s} + \mathrm{n_r},\ i = 1.2.3.\dots.M \tag{1}$$

where the element G indicates the relay R's optoelectronic transformation efficiency R. L_i indicates the optical channel's attenuation coefficient between S_i $(i = 1, 2, 3, \dots M\ )$ & R; and n_r symbolizes the noise at R, which is represented by additive white Gaussian noise (AWGN), and a mean of zero which has a variance noise indicated σ_r^2.

Furthermore, the signal that is transmitted is considered to be symbols that are chosen with a similar likelihood from on-off keying (OOK) constellation such that $x_s \in \{0.2P_t\}$, where P_t represents the average power of the optical signal that is being conveyed. Accordingly, the signal-to-noise ratio (SNR) that was received for ith link can be written as [34]

$$\gamma_i = \frac{2P_t^2 G^2 L_i^2}{\sigma_r^2}\ ,\ i = 1,2,3, \dots, M \tag{2}$$

Presuming the selective transmission technique is employed by the source nodes [40], the maximal γ_i is determined as the first hop's output SNR, which may represented as

$$\gamma_{sr} = max\{\gamma_1.\gamma_2.\dots.\gamma_M\} \tag{3}$$

In second hop, UAV relay R employs the decode-and-forward protocol to decipher obtained signal, and then UAV-relay transmits recoded signal as x_r destination D. Consequently, signal obtained at node D can be expressed as follows

$$y_d = GL_{M+1}x_r + n_d \tag{4}$$

where L_{M+1} denotes the factor associated with channel signal degradation between D and R, and n_d represents the additive white Gaussian noise at D, characterized by a mean of zero and a variance of σ_d^2. Consequently, the signal-to-noise ratio at D can be formulated as

$$\gamma_{rd} = \frac{2P_t^2 G^2 L_{M+1}^2}{\sigma_d^2} \tag{5}$$

Consequently, the SNR of the S to D connect (end-to-end) may be represented as [41]

$$\gamma = min\{\gamma_{sr}.\gamma_{rd}\} \tag{6}$$

Al-Furat Journal of Innovations in Electronics and Computer Engineering (FJIECE)
ISSN -2708-3985

2.2. Channel model

There exist two types of connections within the system under consideration; specifically, the ground-to-UAV (G2U) link connecting S_i to R (where $i = 1.2.3.\dots.M$) and the UAV-to-ground (U2G) link connecting node R to node D. The attenuation coefficient L_i for each link is determined as the product of four distinct factors, expressed as

$$L_i = L_i^t L_i^a L_i^p L_i^{ao} \ , \ i = 1.2.3.\dots.M + 1 \qquad (7)$$

where L_i^t represents the atmospheric turbulence, L_i^a denotes the atmospheric losses, L_i^p designates the pointing errors and L_i^{ao} indicates the AoA fluctuations. The statistical properties of the four factors will be breakdown as follows:

2.2.1 Atmospheric Turbulence

In light of the impact of fading brought on by air turbulence, a Gamma–Gamma (GG) distribution is employed here due to its tight agreement with measurements across a range of turbulence scenarios influencing the propagation of spherical and Gaussian beams. The PDF of L_i^t for the GG model is represented as [42]

$$f_{L_i^t}(L_i^t) = \frac{(\alpha_i\beta_i)^{(\alpha_i+\beta_i)/2} L_i^{t(\alpha_i+\beta_i)/2-1}}{\Gamma(\alpha_i)\Gamma(\beta_i)} G_{0.2}^{2.0}\left(\alpha_i\beta_i L_i^t \left| \frac{\alpha_i-\beta_i}{2}.\frac{\beta_i-\alpha_i}{2} \right.\right) \qquad (8)$$

where α_i and β_i denote parameters that symbolize the fine number of small-scale and large-scale eddies amid atmospheric turbulence, as described reference [43], with $\Gamma(.)$denoting the gamma function.

2.2.2 Atmospheric Loss

The exponential Beers-Lambert law is used to explain loss atmosphere, which is defined as follows [36]

$$L_i^a = exp\,(-Z_i\sigma). \ \ i = 1.2.3.\dots.M + 1 \qquad (9)$$

where Z_i is ith connection distance, σ is the coefficient of atmospheric reduction, which is dependent on visibility situations.

2.2.3 Pointing Error Loss

Assuming a circular detector with a gap radius r_a at receiver, as depicted Figure 2, we can observe impact Gaussian beam on aperture of receiver, which positioned perpendicular to the receiver's lens plane. It is assumed that the displacement vector radially out from the center of the detector to the centroid of the beam is $r_{d.i} = [x_{d.i}. y_{d.i}]$, with $x_{d.i}$ and $y_{d.i}$ representing the displacements along the horizontal and elevation axes at the detector plane, respectively. Therefore, the random variables $x_{d.i}$ and $y_{d.i}$ can be expressed as

$$\begin{aligned} x_{d.i} &= x_{t.i} + x_{r.i} + x_{\theta_{t.i}} = x_{tr.i} + Z_i\theta_{tx.i} \\ y_{d.i} &= y_{t.i} + y_{r.i} + y_{\theta_{t.i}} = y_{tr.i} + Z_i\theta_{ty.i} \end{aligned} \tag{10}$$

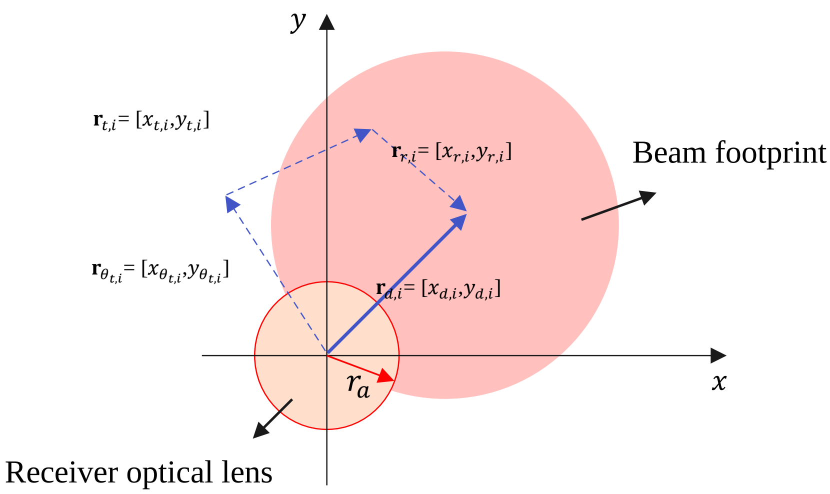

Fig. 2. The impression of the Gaussian beam on the aperture of the receiver.

According to the central limit theorem, the deviations in position and direction resulting from a large number of random events follow Gaussian distributions. The deviations in the position of the transmitter and receiver installed on the UAV are denoted as $(x_{t.M+1}.\ y_{t.M+1}.x_{r.i}$ and $y_{r.i}\ )$ for $i = 1.2.3.,,,.M$, are considered to follow a Gaussian distribution with a mean of zero and a variance of $\sigma_{p.g}^2$. Similarly, for the ground platform, the position deviations $(x_{r.M+1}.\ y_{r.M+1}.x_{t.i}$ and $y_{t.i})$ for $i = 1.2.3.,,,.M$ are likewise considered to be zero-mean Gaussian stochastic variables characterized by a variance of $\sigma_{p.g}^2$. Within the framework of the S to R link, the angular variations $\theta_{tx.i}$, and $\theta_{ty.i}$ are defined as null, whereas $\theta_{tx.M+1}$, and $\theta_{ty.M+1}$ exhibit a zero-mean Gaussian distribution with a variance of σ_o^2. Assuming the independence of the stochastic variables in the displacement equation, the aggregated radial displacement $r_{tr.i} = \sqrt{x_{d.i}^2 + y_{d.i}^2}$ adheres to a Rayleigh distribution, which can be mathematically represented as

$$f_{r_{tr.i}}(r_{tr.i}) = \frac{r_{tr.i}}{\sigma_{s.i}^2} exp\left(-\frac{r_{tr.i}^2}{2\sigma_{s.i}^2}\right) \tag{11}$$

Al-Furat Journal of Innovations in Electronics and Computer Engineering (FJIECE)
ISSN -2708-3985

The overall displacement difference, denoted as $\sigma_{s.i}^2$, for links from S to R is derived as

$$\sigma_{s,i}^2 = \begin{cases} \sigma_{p,g}^2 + \sigma_{p,u}^2, & i = 1,2,3,\dots,M \\ \sigma_{p,g}^2 + \sigma_{p,u}^2 + Z_i^2\sigma_o^2, & i = M+1 \end{cases} \tag{12}$$

Therefore, the PDF representing pointing error can be described as [44]

$$f_{L_i^p}\left(L_i^p\right) = \frac{\xi_i^2}{A_i^{\xi_i^2}}\left(L_i^p\right)^{\xi_i^2-1}, 0 \le L_i^p \le A_i \tag{13}$$

where $\xi_i^2 = \omega_{L_{eq},i}^2/(4\sigma_{s,i}^2)$, $A_i = (erf(v_i))^2$ signifies the maximal portion of the gathered power with $v_i = \sqrt{\pi}r_a/(2\omega_{Z,i}$, $\omega_{Z_{eq},i}^2 = \omega_{Z,i}^2\sqrt{\pi}\,erf(v_i)/(2v_i exp(-v_i^2))$ represents the beam waist counterpart, $\omega_{Z,i}$ represents beam waist at a detachment Z_i, and $erf(\cdot)$ represent mistake function defined as $erf(x) = \frac{2}{\sqrt{\pi}}\int_0^x e^{-t^2}\,dt$.

2.2.4 AoA fluctuation

The angle of arrival variation indicates that the laser beam is not perpendicular to the receiver plane when it intersects it. An arriving laser beam with an angle of arrival, represented by $\theta_{a.i}$, may sometimes surpass the detection range because of significant orientation variations in the hovering position of the UAV. An outage will happen if AoA received exceeds field of vision. Consequently, the angle of arrival of the signal is determined as $\theta_{a.i} = \sqrt{\theta_{tx.i}^2 + \theta_{ty.i}^2}$, which follows with a Rayleigh distribution represented as [45]

$$f_{\theta_{a.i}}(\theta_{a.i}) = \frac{\theta_{a.i}}{\sigma_o^2}exp\left(-\frac{\theta_{a.i}^2}{2\sigma_o^2}\right).\ \ \theta_{a.i} \ge 0 \tag{14}$$

The connection between the transmitter and receiver (S and R) is interrupted when the angle of arrival of the received beam falls outside of the field of view (FoV). Therefore, the function L_i^{ao} can be defined as

$$L_i^{ao} = \begin{cases} 1.\,if\ \ \theta_{a.i} \le \theta_{FoV.i} \\ 0.\,if\ \ \theta_{a.i} > \theta_{FoV.i} \end{cases} \tag{15}$$

where $\theta_{FoV,i}$ is the field of view of the ith receiver. Hence, from (14) and (15), the PDF of L_i^{ao} can be written as

$$f_{L_i^{ao}}(L_i^{ao}) = \exp\left(-\frac{\theta_{FoV,i}^2}{2\sigma_o^2}\right)\delta(L_i^{ao}) + \left[1 - \exp\left(-\frac{\theta_{FoV,i}^2}{2\sigma_o^2}\right)\right]\delta(L_i^{ao} - 1) \tag{16}$$

where $\delta(.)$ is the Delta function in Dirac theory. Combining the GG distribution for atmospheric turbulence , with factors such as path losses, pointing errors, and AoA losses specific to the system being studied the creates a new PDF model.

Subsequently, we derive the Probability Density Function and the Cumulative Distribution Function (CDF) for the consolidated channel model by integrating the comprehensive atmospheric

Al-Furat Journal of Innovations in Electronics and Computer Engineering (FJIECE)
ISSN -2708-3985

turbulence framework with atmospheric degradation, pointing inaccuracies, and AoA losses associated with the FSO systems deployed on UAVs.

2.3. Unified channel Model

As per the four factors, the PDF of L_i can be represented

$$f_{L_i}(x) = \int_0^\infty \frac{1}{L_i} f_{L_i^{ao}}\left(\frac{x}{L_i}\right) f_{L_i}(L_i) dL_i \tag{17}$$

where $L_i = L_i^t L_i^a L_i^p L_i^{ao}$. Furthermore, the PDF can be obtained as

$$f_{L_i}(x) = \int_0^\infty f_{x/L_i^{ao}}\left(\frac{x}{L_i^{ao}}\right) f_{L_i^{ao}}(L_i^{ao}) dL_i^{ao} \tag{18}$$

By incorporating (8), (9), (13), and (16) in (18) and applying ([46], Eq. (9.31.5)), the unified PDF of L_i is obtained as

$$\begin{aligned} f_{L_i}(x) &= exp\left(-\frac{\theta_{FoV,i}^2}{2\sigma_o^2}\right)\delta(L_i) + \left[1 - exp\left(-\frac{\theta_{FoV,i}^2}{2\sigma_0^2}\right)\right] \\ &\times \frac{\alpha_i\beta_i}{A_i L_i^{a0}\Gamma(\alpha_i)\Gamma(\beta_i)} G_{1,3}^{3,0}\left(\frac{\alpha_i\beta_i}{A_i L_i^{ao}} x \middle| \begin{matrix} \xi_i^2 \\ \xi_i^2 - 1, \alpha_i - 1, \beta_i - 1 \end{matrix}\right) \end{aligned} \tag{19}$$

where $G_{p,q}^{m,n}[\cdot]$ is Meijer's G-function.

3. PERFORMANCE ANALYSIS

The average bit error rate performance of the UAV-based FSO system using OOK modulation is determined as described [47]

$$\begin{aligned} P_b(x) &= \mathbb{E}\left[\frac{1}{2} erfc\left(\sqrt{\frac{\gamma_0 x^2}{4}}\right)\right] \\ &= \frac{1}{2\sqrt{\pi}} \int_0^\infty G_{1,2}^{2,0}\left(\frac{\gamma_i x^2}{4} \middle| \begin{matrix} 1 \\ 1,0.5 \end{matrix}\right) f_{L_i}(x) dx \end{aligned} \tag{20}$$

In (20), the complementary error function, designated as erfc(,), is employed ([46], Eq. (8.250.4)) and is articulated employing Meijer's G-function [[46], Eq. (8.4.14.1)]. By incorporating (19) into (20) and utilizing the integration formula from [[48], Eq. (07.34.21.0084.01)], we derive a closed form representation to the average BER of the system under examination as

$$P_b(x) = \frac{1}{2\sqrt{\pi}}\left[exp\left(-\frac{\theta_{FoV.i}^2}{2\sigma_o^2}\right)\delta(L_i^{ao})G_{2.3}^{2.1}\left(\frac{\sigma_{sr}^2}{8\eta^2 P_t^2}\middle|\begin{matrix}1.2\\2.1,5.0\end{matrix}\right)\right.$$
$$\left.+\psi_i G_{5.4}^{2.4}\left(\frac{\alpha_i\beta_i\sigma_{sr}^2}{16A_iL_i^a\eta^2P_t^2}\middle|\begin{matrix}1.\xi_i^2.\frac{-\xi_i^2+2}{2}.\frac{-\alpha_i-2}{2}.\frac{-\beta_i-2}{2}\\ \xi_i^2-1.\alpha_i-1.\beta_i-1.\frac{-\xi_i^2}{2}.\end{matrix}\right)\right] \quad (21)$$

where $\psi_i = \frac{\alpha_i\beta_i\left[1-exp\left(-\frac{\theta_{FoV,i}^2}{2\sigma_0^2}\right)\right]}{2(\pi)^{3/2}A_iL_i^a\Gamma(\alpha_i)\Gamma(\beta_i)}$.

4. NUMERICAL RESULTS

In this section, computational methodologies alongside Monte Carlo simulations (averaged over 10^8 channel realizations) are employed to assess the effectiveness of the UAV-centric free-space optical communication framework and to validate the accuracy of the derived theoretical models. Additionally, a thorough examination is performed to investigate the influence of various system parameters on the error probability, presuming uniform distances between the source and relay, as well as between the relay and recipient. The simulation parameters used for clarity are elaborated in Table 1. This simulation was executed using MATLAB.

Table 1. Simulation Parameters.

Parameter	Values
Wavelength, λ	1550 nm
Bandwidth, B	250 MHz
Index of refraction structure parameter, C_n^2	2.5×10^{-14} m$^{-2/3}$
Data rate, R	4000 Mbits/s
Optoelectronic conversion factor, η	0.9
Noise variance at R, σ_r^2	2.5×10^{-14}
Noise variance at D, σ_{rd}^2	2.5×10^{-14}
FoV of the ith Rx, θ_{FoV}	5 mrad
Aperture radius, a_r	25×10^{-3} m
Atmospheric attenuation coefficient, σ	$0.001m^{-1}$
The standard deviation of the UAV displacement, $\sigma_{p,u}$	10cm
The standard deviation of the ground displacement, $\sigma_{p,g}$	10cm
The variance of the orientation deviations, σ_o	1.2 mrad
Beam waist at Z_i, $\omega_{Z,i}$	2m
α, β	3.01, 3

Al-Furat Journal of Innovations in Electronics and Computer Engineering (FJIECE)
ISSN -2708-3985

Figures 3, 4, and 5 illustrate the BER of analyzed system in relation to the quantity of users M =3 and $\sigma^2_{R.i}$ = 0.5 under various rainy weather conditions characterized by different propagation distances and minimal pointing error losses. Initially, it was observed that the BER decreased with an increase in transmission power across all weather scenarios. Furthermore, an extended distance (Z_i = 2000) correlates with an elevated BER, as both path loss and signal degradation intensify with increased distance. In this context, signal absorption phenomena and scattering, particularly under weighty rainfall over lengthy distances, contribute to the heightened BER. While absorption and scattering diminish during light rain and moderate, the prolonged distance influences the BER. Conversely, for a shorter distance (Z_i = 100), the briefer distance reduces the extent showing signal deterioration when the optical beam goes through a smaller rain volume of rain, resulting in decreased absorption and scattering; thereby, the BER is to decline.

Figure 6 illustrates the impact of distance on the average bit error rate when the pointing error constant is set at $\xi = 6{,}7$. The results show that the BER increases as transmission distances increase. However, when the distance is at Z_i = 100, the system's performance improves, leading to a reduction in BER. In summary, as distance increases, the BER rises.

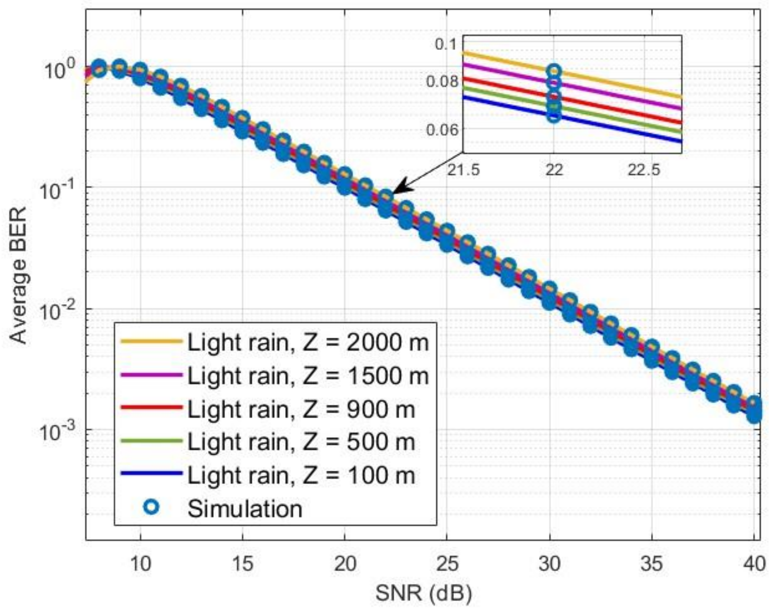

Fig. 3. BER performance versus SNR during light rain and different distances when $\sigma^2_{R,i} = 0.5$ and $M = 3$.

Al-Furat Journal of Innovations in Electronics and Computer Engineering (FJIECE)
ISSN -2708-3985

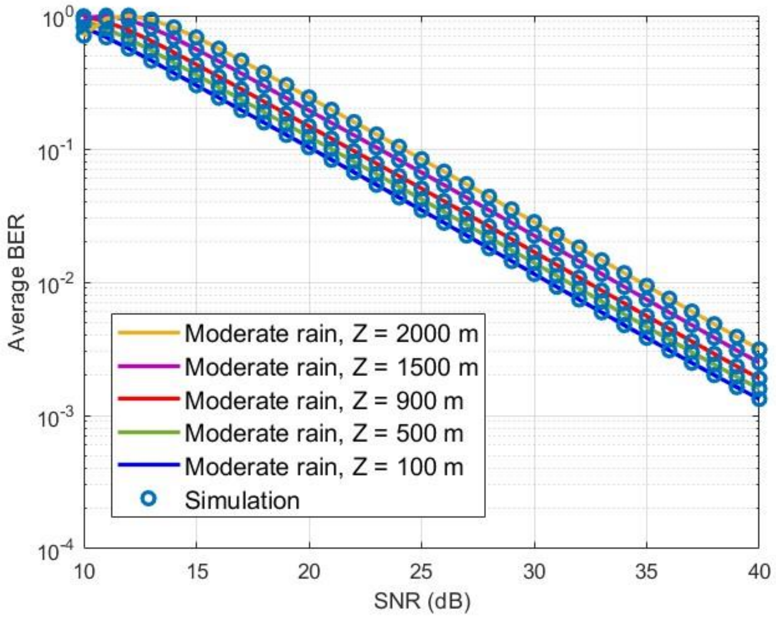

Fig. 4. BER performance versus SNR during moderate rain and different distances when $= 0.5$ and $M = 3$.

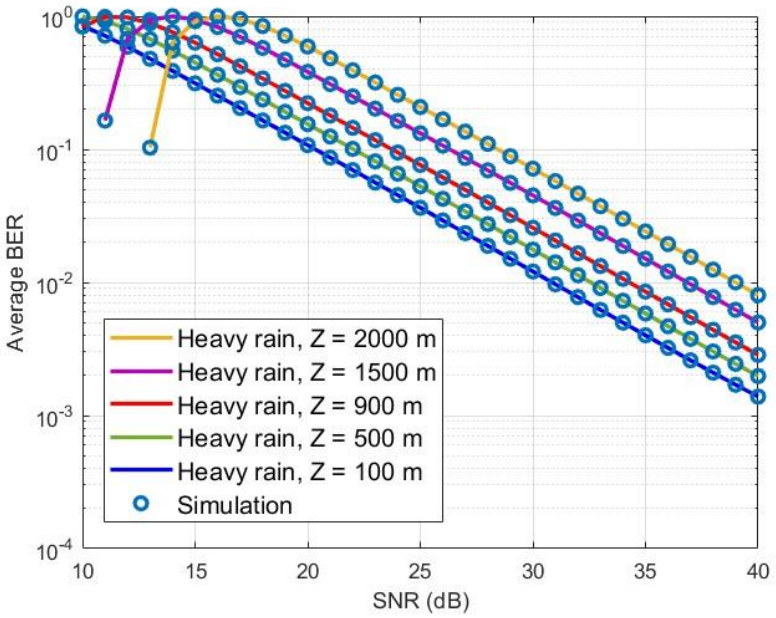

Fig. 5. BER performance versus SNR during heavy rain and different distances when $\sigma_{R,i}^2 = 0.5$ and $M = 3$.

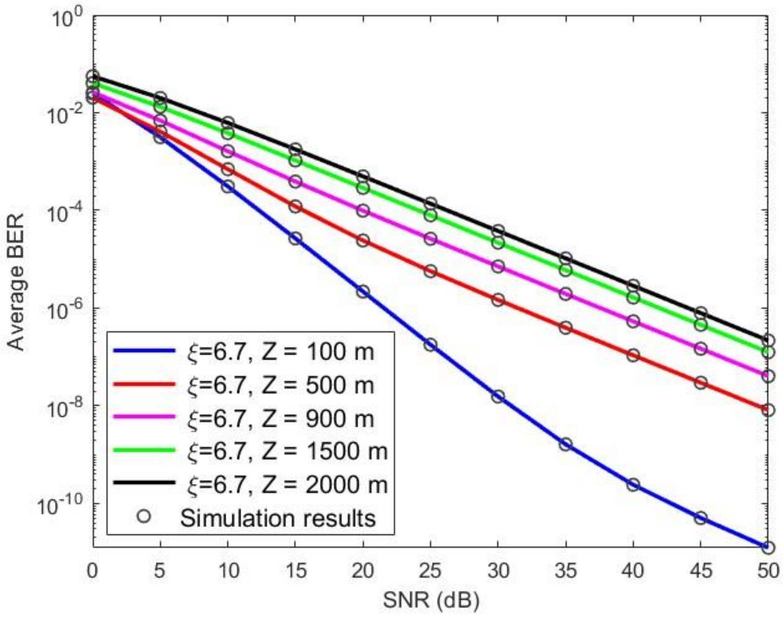

Fig. 6. Average BER against the SNR for varying distances.

5. CONCLUSION

This research scrutinized the integrated channel model and performed a comprehensive performance assessment dual-hop architecture for UAV-enabled FSO communication involving multiple sources. The extensive analytical results allow for the evaluation of the UAV-based FSO system underneath different atmospheric circumstances, particularly when applying the GG turbulence model. This assessment considers elements like variations in the AOA, atmospheric losses, and pointing errors. We have established a precise analytical expression for the system's BER. The numerical analyses performed confirm the accuracy of our theoretical models. These models enable system architects to effectively evaluate the performance of these systems without the requirement for costly and time-intensive simulations. Furthermore, our understanding of factors that impact BER performance enables system designers to specify optimal choices among the various parameters.

REFERENCES

[1] W. M. R. Shakir, "On secrecy performance of multiuser FSO networks with opportunistic user scheduling," *2021 International Symposium on Networks, Computers and Communications (ISNCC)*, Dubai, United Arab Emirates, pp. 1-6 , 2021, doi: 10.1109/ISNCC52172.2021.9615862.S.

[2] S. A. A. Mohammed, W. M. R. Shakir, and A. A. Hilli, "Security-Reliability Analysis of FSO Communications Over Generalized F Channel," in *IEEE Al-Sadiq International Conference on Communication and Information Technology (AICCIT)*, pp. 304–309 ,2023. doi: 10.1109/AICCIT57614.2023.10218177.

[3] R. A. Kareem and W. Shakir, “On secrecy capacity analysis of FSO communication systems under generalized Malaga-M turbulence,” *AIP Conf. Proc.*, vol. 2834, no. 1, p. 50036, Dec. 2023, doi: 10.1063/5.0161615.

[4] W. M. R. Shakir *et al.*, "Novel Approximate Distribution of the Generalized Turbulence Channels for MIMO FSO Communications," in *IEEE Photon. J.*, vol. 16, no. 4, pp. 1-15, Aug. 2024, Art no. 7302715, doi: 10.1109/JPHOT.2024.3418371.

[5] W. M. R. Shakir, J. Charafeddine, H. A. Satai, H. Hamdan, S. Haddad and J. Sayah, "Opportunistic Schedule selection for multiuser MIMO FSO communications: A security- reliability trade-off perspective," in *IEEE Photon. J.l*, vol. 15, no. 3, pp. 1-15, June 2023, Art no. 7900215, doi: 10.1109/JPHOT.2023.3262183..

[6] H. Z. Dhaam, Z. J. Al-Allaq, and M. J. Al_Dujaili, “Multicarrier millimeter wave through wireless optical communication,” in *AIP Conference Proceedings*, AIP Publishing, 2024.

[7] W. Shakir and R. Abdulkareem, “A survey on physical layer security for FSO communication systems,” in *Proceedings of 2nd International Multi-Disciplinary Conference Theme: Integrated Sciences and Technologies, IMDC-IST 2021, 7-9 September 2021, Sakarya, Turkey*, 2022.

[8] E. Zedini, H. Soury, and M.-S. Alouini, “On the Performance Analysis of Dual-Hop Mixed FSO/RF Systems,” *IEEE Trans. Wirel. Commun.*, vol. 15, no. 5, pp. 3679–3689, 2016, doi: 10.1109/TWC.2016.2524685.

[9] A. J. Aljohani, J. Mirza, and S. Ghafoor, “A Novel Regeneration Technique for Free Space Optical Communication Systems,” *IEEE Commun. Lett.*, vol. 25, no. 1, pp. 196–199, 2021, doi: 10.1109/LCOMM.2020.3029591.

[10] D. Chadha, *Terrestrial wireless optical communication*. McGraw Hill Professional, 2013.

[11] W. M. R. Shakir and S. A. A. Mohammed, “Free Space Optical Communications Security and Reliability Trade-off: A Survey,” in *2022 International Conference for Natural and Applied Sciences (ICNAS)*, pp. 114–119 ,2022. doi: 10.1109/ICNAS55512.2022.9944674.

[12] J.-Y. Wang, J.-B. Wang, M. Chen, Y. Tang, and Y. Zhang, “Outage Analysis for Relay-Aided Free-Space Optical Communications Over Turbulence Channels With Nonzero Boresight Pointing Errors,” *IEEE Photonics J.*, vol. 6, no. 4, pp. 1–15, 2014, doi: 10.1109/JPHOT.2014.2332554.

[13] E. Zedini, H. Soury, and M.-S. Alouini, “Dual-Hop FSO Transmission Systems Over Gamma–Gamma Turbulence With Pointing Errors,” *IEEE Trans. Wirel. Commun.*, vol. 16, no. 2, pp. 784–796, 2017, doi: 10.1109/TWC.2016.2630680.

[14] C. Abou-Rjeily and W. Fawaz, “Buffer-Aided Serial Relaying for FSO Communications: Asymptotic Analysis and Impact of Relay Placement,” *IEEE Trans. Wirel. Commun.*, vol. 17, no. 12, pp. 8299–8313, 2018, doi: 10.1109/TWC.2018.2875979.

[15] N. A. Mohd Nor *et al.*, “Experimental analysis of a triple-hop relay-assisted FSO system with turbulence,” *Opt. Switch. Netw.*, vol. 33, pp. 194–198, 2019, doi: https://doi.org/10.1016/j.osn.2017.11.002.

[16] S. Althunibat, Z. Altarawneh, and R. Mesleh, “Performance analysis of free space optical–based wireless sensor networks using corner cube retroreflectors,” *Trans. Emerg. Telecommun. Technol.*, vol. 30, no. 12, p. e3707, Dec. 2019, doi: https://doi.org/10.1002/ett.3707.

[17] N. A. M. Nor, M. Komanec, J. Bohata, Z. Ghassemlooy, M. R. Bhatnagar, and S. Zvánovec, “Experimental all-optical relay-assisted FSO link with regeneration and forward scheme for ultra-short pulse transmission,” *Opt. Express*, vol. 27, no. 16, pp. 22127–22137, 2019, doi: 10.1364/OE.27.022127.

[18] S. Zvanovec, J. Perez, Z. Ghassemlooy, S. Rajbhandari, and J. Libich, “Route diversity analyses for free-space optical wireless links within turbulent scenarios,” *Opt. Express*, vol. 21, no. 6, pp. 7641–7650, 2013, doi: 10.1364/OE.21.007641.

[19] Z. J. Al-Allaq and W. M. R. Shakir, "A Comprehensive Analysis of FSO Communications with UAV Technologies," *2024 International Symposium on Networks, Computers and Communications (ISNCC)*, Washington DC, DC, USA, pp. 1-7 ,2024 , doi: 10.1109/ISNCC62547.2024.10758984.

[20] R. Ara, I. E. Lee, Z. Ghassemlooy, G. C. Chung, and W. L. Pang, “Error Performance of Relay-Assisted Free-Space Optical Communication Links Over Atmospheric Turbulence Channels,” in *International Congress on Information and Communication Technology*, Springer, pp. 25–37,2024. doi: 10.1007/978-981-99-3043-2_3.

[21] W. Fawaz, C. Abou-Rjeily, and C. Assi, “UAV-Aided Cooperation for FSO Communication Systems,” *IEEE Commun. Mag.*, vol. 56, no. 1, pp. 70–75, Jan. 2018, doi: 10.1109/MCOM.2017.1700320.

[22] F. Yang, J. Cheng, and T. A. Tsiftsis, “Free-space optical communication with nonzero boresight pointing errors,” *IEEE Trans. Commun.*, vol. 62, no. 2, pp. 713–725, 2014.

[23] M. Alzenad, M. Z. Shakir, H. Yanikomeroglu, and M.-S. Alouini, “FSO-based vertical backhaul/fronthaul framework for 5G+ wireless networks,” *IEEE Commun. Mag.*, vol. 56, no. 1, pp. 218–224, 2018.

[24] Y. Dong, M. Z. Hassan, J. Cheng, M. J. Hossain, and V. C. M. Leung, “An Edge Computing Empowered Radio Access Network with UAV-Mounted FSO Fronthaul and Backhaul: Key Challenges and Approaches,” *IEEE Wirel. Commun.*, vol. 25, no. 3, pp. 154–160, 2018, doi: 10.1109/MWC.2018.1700419.

[25] G. Xu, N. Zhang, M. Xu, Z. Xu, Q. Zhang, and Z. Song, “Outage Probability and Average BER of UAV-Assisted Dual-Hop FSO Communication With Amplify-and-Forward Relaying,” *IEEE Trans. Veh. Technol.*, vol. 72, no. 7, pp. 8287–8302, Jul. 2023, doi: 10.1109/TVT.2023.3252822.

[26] J.-H. Lee, K.-H. Park, Y.-C. Ko, and M.-S. Alouini, “Throughput Maximization of Mixed FSO/RF UAV-Aided Mobile Relaying With a Buffer,” *IEEE Trans. Wirel. Commun.*, vol. 20, no. 1, pp. 683–694, Jan. 2021, doi: 10.1109/TWC.2020.3028068.

[27] A. Kaadan, H. Refai, and P. Lopresti, “Spherical FSO receivers for UAV communication: geometric coverage models,” *IEEE Trans. Aerosp. Electron. Syst.*, vol. 52, no. 5, pp. 2157–2167, 2016, doi: 10.1109/TAES.2016.150346.

[28] A. Kaadan, H. H. Refai, and P. G. LoPresti, “Multielement FSO Transceivers Alignment for Inter-UAV Communications,” *J. Light. Technol.*, vol. 32, no. 24, pp. 4785–4795, 2014, doi: 10.1109/JLT.2014.2364795.

[29] H. Ajam, M. Najafi, V. Jamali, and R. Schober, “Ergodic Sum Rate Analysis of UAV-Based Relay Networks With Mixed RF-FSO Channels,” *IEEE Open J. Commun. Soc.*, vol. 1, pp. 164–178, 2020, doi: 10.1109/OJCOMS.2020.2969492.

[30] M. Najafi, H. Ajam, V. Jamali, P. D. Diamantoulakis, G. K. Karagiannidis, and R. Schober, “Statistical Modeling of the FSO Fronthaul Channel for UAV-Based Communications,” *IEEE Trans. Commun.*, vol. 68, no. 6, pp. 3720–3736, 2020, doi: 10.1109/TCOMM.2020.2981560.

[31] S. Huang and M. Safari, “Free-Space Optical Communication Impaired by Angular Fluctuations,” *IEEE Trans. Wirel. Commun.*, vol. 16, no. 11, pp. 7475–7487, 2017, doi: 10.1109/TWC.2017.2749219.

[32] V. V Mai and H. Kim, “Beam Size Optimization and Adaptation for High-Altitude Airborne Free-Space Optical Communication Systems,” *IEEE Photonics J.*, vol. 11, no. 2, pp. 1–13, Apr. 2019, doi: 10.1109/JPHOT.2019.2901952.

[33] M. T. Dabiri, S. M. S. Sadough, and M. A. Khalighi, “Channel Modeling and Parameter Optimization for Hovering UAV-Based Free-Space Optical Links,” *IEEE J. Sel. Areas Commun.*, vol. 36, no. 9, pp. 2104–2113, Sep. 2018, doi: 10.1109/JSAC.2018.2864416.

[34] M. T. Dabiri, S. M. S. Sadough, and I. S. Ansari, “Tractable Optical Channel Modeling Between UAVs,” *IEEE Trans. Veh. Technol.*, vol. 68, no. 12, pp. 11543–11550, Dec. 2019, doi: 10.1109/TVT.2019.2940226.

[35] M. T. Dabiri and S. M. S. Sadough, “Optimal Placement of UAV-Assisted Free-Space Optical Communication Systems With DF Relaying,” *IEEE Commun. Lett.*, vol. 24, no. 1, pp. 155–158, 2020, doi: 10.1109/LCOMM.2019.2949274.

[36] J.-Y. Wang, Y. Ma, R.-R. Lu, J.-B. Wang, M. Lin, and J. Cheng, “Hovering UAV-Based FSO Communications: Channel Modelling, Performance Analysis, and Parameter Optimization,” *IEEE J. Sel. Areas Commun.*, vol. 39, no. 10, pp. 2946–2959, Oct. 2021, doi: 10.1109/JSAC.2021.3088656.

[37] H. Safi, A. Dargahi, and J. Cheng, “Beam Tracking for UAV-Assisted FSO Links With a Four-Quadrant Detector,” *IEEE Commun. Lett.*, vol. 25, no. 12, pp. 3908–3912, Dec. 2021, doi: 10.1109/LCOMM.2021.3113699.

[38] Z. J. Al-Allaq, H. Z. Dhaam, M. J. A. D. Al-Khazraji, and M. H. I. Al-Khuzaie, “Discovering the spatial locations of the radio frequency radiations effects around mobile towers,” *Int. J. Electr. Comput. Eng.*, vol. 13, no. 2, p. 1629, Apr. 2023, doi: 10.11591/ijece.v13i2.pp1629-1638.

[39] S. Song, M. Choi, D.-E. Ko, and J.-M. Chung, “Multi-UAV Trajectory Optimization Considering Collisions in FSO Communication Networks,” *IEEE J. Sel. Areas Commun.*, vol. 39, no. 11, pp. 3378–3394, Nov. 2021, doi: 10.1109/JSAC.2021.3088665.

[40] W. M. R. Shakir, “On Secrecy Performance of Multiuser FSO Networks with Opportunistic User Scheduling,” in *2021 International Symposium on Networks, Computers and Communications (ISNCC)*, IEEE, pp. 1–6., Oct 2021.doi: 10.1109/ISNCC52172.2021.9615862.

[41] Z. Dan, X. Wu, S. Zhu, T. Zhuang, and J.-Y. Wang, “On the Outage Performance of Dual-Hop UAV Relaying with Multiple Sources,” in *2019 Cross Strait Quad-Regional Radio Science and Wireless Technology Conference (CSQRWC)*, IEEE, pp. 1–3., Jul. 2019.doi: 10.1109/CSQRWC.2019.8799304.

[42] T. V. Pham, T. C. Thang, and A. T. Pham, “Average Achievable Rate of Spatial Diversity MIMO-FSO Over Correlated Gamma–Gamma Fading Channels,” *J. Opt. Commun. Netw.*, vol. 10, no. 8, pp. 662–674, Aug. 2018, doi: 10.1364/JOCN.10.000662.

[43] W. M. R. Shakir, “Performance evaluation of diversity combining scheme for the hybrid FSO/RF system,” in *2017 IEEE 2nd Information Technology, Networking, Electronic and Automation Control Conference (ITNEC)*, IEEE, pp. 984–989, Dec. 2017. doi: 10.1109/ITNEC.2017.8284884.

[44] W. M. R. Shakir, J. Charafeddine, H. Al Satai, H. Hamdan, S. Haddad, and J. Sayah, “Opportunistic Schedule Selection for Multiuser MIMO FSO Communications: A Security-Reliability Trade-Off Perspective,” *IEEE Photonics J.*, vol. 15, no. 3, pp. 1–15, Jun. 2023, doi: 10.1109/JPHOT.2023.3262183.

[45] R.-R. Lu, J.-Y. Wang, X.-T. Fu, S.-H. Lin, Q. Wang, and B. Zhang, “Performance analysis and optimization for UAV-based FSO communication systems,” *Phys. Commun.*, vol. 51, p. 101594, Apr. 2022, doi: 10.1016/j.phycom.2021.101594.

[46] I. S. G. and I. M. Ryzhik, *Table of integrals, series, and products*, 7th ed. Burlington, MA, USA: Elsevier, 2007.

[47] E. Bayaki, R. Schober, and R. K. Mallik, “Performance analysis of MIMO free-space optical systems in gamma-gamma fading,” *IEEE Trans. Commun.*, vol. 57, no. 11, pp. 3415–3424, Nov. 2009, doi: 10.1109/TCOMM.2009.11.080168.

[48] Wolfram Research, Inc., “The Wolfram functions site.” [Online]. Available: https://functions.wolfram.com/HypergeometricFunctions/M%0AeijerG/ 21/02/03/01/0002/.